JOC The Journal of Organic Chemistry

Article

pubs.acs.org/joc

A Non-Karplus Effect: Evidence from Phosphorus Heterocycles and DFT Calculations of the Dependence of Vicinal Phosphorus–Hydrogen NMR Coupling Constants on Lone-Pair Conformation

William H. Hersh,* Sherrell T. Lam, Daniel J. Moskovic, and Antonios J. Panagiotakis

Department of Chemistry and Biochemistry, Queens College and the Graduate Center of the City University of New York, Flushing, New York 11367-1597, United States

Supporting Information

ABSTRACT: In contrast to literature reports of a Karplus-type curve that correlates $^3J_{PH}$ with phosphorus–hydrogen dihedral angle, a recently reported glycine-derived 1,3,2-oxazaphospholidine (**7c**) has two hydrogen atoms on the ring with identical PNCH dihedral angles but measured coupling constants of ~6 and 1.5 Hz. DFT calculations were in accord with these values and suggested that the smaller coupling constant is negative. Experimental evidence of the opposite signs of these coupling constants was obtained by analysis of the ABX NMR spectrum of the new glycine-derived *N*-*p*-toluenesulfonyl phosphorus heterocycle **6c**. DFT calculations on **6c** and on Me_2NPCl_2 and *t*-$BuPCl_2$ were also in accord with NMR data and allowed confirmation of unusual features including a lone pair effect on $^3J_{PH}$, the negative coupling constant, temperature-dependent chemical shifts due to rotation about the sulfonamide S–N bond, and vicinal phosphorus–hydrogen coupling constants over 40 Hz. Calculation of phosphorus–hydrogen coupling constants both as a function of PYCH dihedral angle θ (Y = O, N, C) and lone pair-PYC dihedral angle ω shows similar θ,ω surfaces for $^3J_{PH}$ with a range of $^3J_{PH}$ from −4.4 to +51 Hz and demonstrates the large non-Karplus effect of lone-pair conformation on vicinal phosphorus–hydrogen coupling constants.

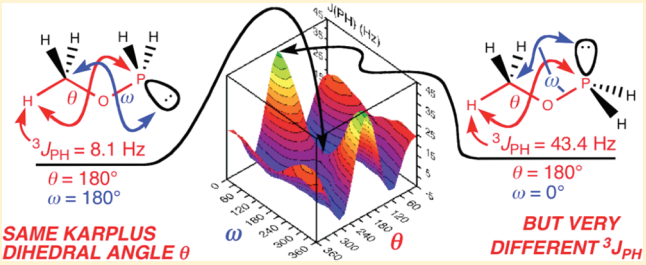

The use of the Karplus equation to estimate torsional angles from vicinal proton–proton coupling constants is a staple of organic structure determination. At its inception,[1] the Karplus equation giving $^3J_{HH}$ as a function of $\cos^2\theta$ was introduced as a simple approximation of the theoretically calculated coupling constants, not as a fit of a curve to observed NMR data. However, the approximation was noted to be in accord with experimental data.[1,2]

Several groups soon showed in qualitative fashion that vicinal phosphorus–hydrogen coupling constants exhibited a similar dependence on dihedral angle in phosphonates,[3,4] a thiophosphoryl dichloride,[5] phosphites,[6−8] and phosphate triesters[7] and for phosphate diesters[9−11] developed quantitative Karplus equations such as that shown in eq 1:[11]

$$^3J_{POCH} = 15.3\cos^2\theta - 6.1\cos\theta + 1.6 \quad (1)$$

Unlike the original Karplus equation, the coefficients were the best-fit parameters to a small number of *experimental* rather than *theoretical* data points, and eq 1 was assumed to be the correct shape that allowed interpolation and extrapolation from the known values of $^3J_{POCH}$ and θ. Such correlations have now been used for years, most frequently for analysis of oligonucleotide conformations[12,13] but for other phosphates as well.[14,15]

In contrast to this empirical fitting approach and in a return to the original Karplus method,[1] Giessner-Prettre and Pullman reported the use of molecular orbital calculations to calculate vicinal coupling constants in the nucleotide model compound ethyl phosphate as a function of the POCH (θ) and (HO)POC (ω) dihedral angles (**1**, Figure 1).[16,17] Surprisingly, $^3J_{POCH}$ was found to vary significantly with ω and, except for ω = 180°, was also not completely symmetrical with respect to θ = 180°, unlike eq 1. From the latter finding the authors concluded that ω must be nearly constant in oligonucleotides, since otherwise the simple Karplus equation would not suffice.

Karplus equations have only rarely been proposed for trivalent phosphorus compounds,[18,19] despite the Karplus-type graphs of $^3J_{PH}$ versus θ that have been published.[6−8] The existence of these Karplus equations is curious because there have been many reports going back to that in 1966 by Gagnaire[20] that explicitly noted the effect of lone pair conformation on $^3J_{PH}$.[19−31] For instance in two early examples (Figure 1), cooling **2**[23] and **3**[25,26] to −120 and −140 °C, respectively, gave rise to slow rotation about the P–N and P–C bonds on the NMR time scale, and both compounds exhibited methyl doublets with $^3J_{PH} \approx 20$ Hz for the methyl groups that were gauche to the phosphorus lone pair, but only ~5 Hz for the methyl anti to the lone pair. In both **2** and **3**, the "Karplus" PYCH (Y = N, C) dihedral angles were the same for all methyl

Received: February 22, 2012
Published: May 21, 2012

   dx.doi.org/10.1021/jo3003776 | J. Org. Chem. 2012, 77, 4968–4979

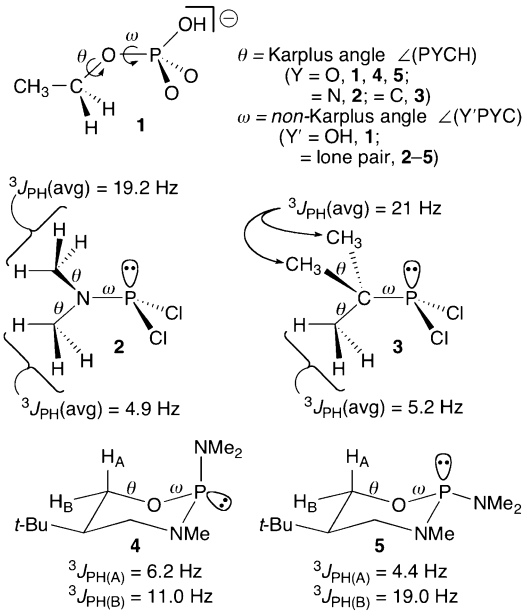

Figure 1. Examples of the effect of P-OH and P-lone pair conformation on Karplus $^3J_{PH}$ coupling constants. For **2** and **3**, $^3J_{PH}$ is the rotationally averaged coupling constant for the methyl group hydrogens.

groups (albeit averaged for methyl rotation), and so it was suggested that the difference must be due to the lone pair orientation. In a more recent example (Figure 1), **4** and **5** must have nearly identical Karplus angles for $POCH_A$ ($\theta \approx 60°$) and $POCH_B$ ($\theta \approx 180°$), yet as shown the coupling constants for equatorial H_B differ significantly for **4** and **5**.[32] For structures such as **5** with the axial lone pair gauche to the C–H carbon, this unusually large ~20 Hz coupling constant for the equatorial vicinal hydrogen is the norm.[30,31] Similarly in **2** and **3**, a large vicinal PH coupling constant is seen when the lone pair is gauche to the PYCH carbon atom. The effect was also noted in a review by Gil and von Philipsborn on the effect of lone pairs on spin–spin coupling constants, although their focus was on one- and two-bond coupling constants;[33] in the 20 years since that review, there does not seem to have been any further comprehensive work on the vicinal case.

We recently reported the syntheses of chiral 1,3,2-oxazaphospholidines from *N*-*p*-toluenesulfonyl (**6**) and *N*-*tert*-butoxycarbonyl (Boc) derivatives of valine and alanine with $PhPCl_2$; the achiral heterocycle **7c** was also prepared from the Boc derivative of glycine (**6** and **7**, Figure 2).[34−36] While there is a long history of related syntheses of amino acid derived heterocycles,[37−43] until our work there were no reports of diastereoselectivity, and so one focus of our analysis was the proof of relative stereochemistry of the ring substituents. This was done using a combination of X-ray and NMR methods. For analogues of **6**, all of the cis isomers exhibited $^3J_{PH}$ = 3.4–3.7 Hz, and all of the trans isomers exhibited $^3J_{PH}$ = 1.4–1.8 Hz. For analogues of **7**, only the trans isomers were observed, and these exhibited $^3J_{PH}$ = 0.9–1.5 Hz. Synthesis of glycine analogue **7c** allowed the "cis" vicinal coupling constant to be measured, however, and it was found to be ~6 Hz.

Precedent for using such coupling constants to determine stereochemistry was provided by prior extensive NMR and X-ray studies of five-membered ring phosphorus heterocycles with tetravalent phosphorus,[45,46] and six-membered ring phosphorus heterocycles with trivalent phosphorus.[19,32] In both cases,

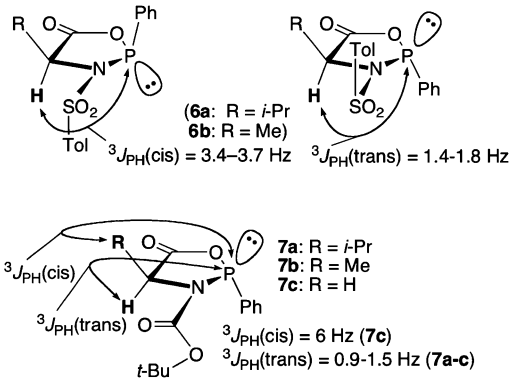

Figure 2. Examples of cis and trans $^3J_{PH}$ in phosphorus amino acid derived heterocycles; the H stereochemistry is defined with respect to the phosphorus lone pair.[35] The amide stereochemistry shown about the C–N bond of **7** is *Z*.[35,44]

POCH but not PNCH coupling constants could be used to determine stereochemistry via Karplus relationships with coupling constants <1 Hz for dihedral angles near 90° and 3–6.5 Hz for dihedral angles near 140° in the five-membered rings and ~12 Hz for dihedral angles approaching 180° in the six-membered rings;[19,46,47] however, for the six-membered ring phosphorinanes (such as **4**, **5**), the Karplus approach was only successful with the phosphorus substituent axial and the lone pair equatorial (as in **4**).[19]

For a variety of reasons, including the anomalously large PH coupling constants of ~20 Hz seen in Figure 1, particularly as a function of phosphorus lone pair orientation, and the differing degrees of utility of PNCH coupling constants, a re-evaluation of phosphorus–hydrogen vicinal coupling constants seemed to be in order. In this paper, we examine in detail the dependence of this coupling on factors other than the Karplus PYCH dihedral angle θ (Y = O, N, C). Using X-ray and observed NMR data as a starting point, we report here (1) a simple experimental case that demonstrates that lone pair conformation in a trivalent phosphorus compound gives rise to *different* vicinal P–H coupling constants despite virtually *identical* Karplus PNCH dihedral angles, (2) deceptively simple-looking variable temperature NMR spectra that show the small trans vicinal coupling constant in an analogue of **6** and **7** to be of opposite sign to the larger cis vicinal coupling constant, (3) the validity of using structures and P–H coupling constants calculated using density functional theory (DFT) methods, including the re-examination of the NMR spectra of **2** and **3** using DFT, which provides experimental as well as theoretical evidence of $^3J_{PH}$ values that exceed 40 Hz, (4) a comparison of different basis sets for calculation of $^3J_{PH}$, and (5) the use of DFT calculations on simple model compounds in order to explore the dependence of vicinal P–H coupling constants on the Karplus dihedral angle of the vicinal atoms and on the non-Karplus lone pair conformation.

RESULTS

Planar *N*-Boc Heterocycles. We recently reported the X-ray crystal structure of the *N*-Boc-substituted 1,3,2-oxazaphospholidinone **7a** (Figure 2).[35] Unlike typical *N*-alkyl 1,3,2-oxazaphospholidines that adopt an envelope conformation,[36,45,46] the *N*-Boc derivative is planar, resulting from the presence of two sp^2 centers in the ring, namely, the ring carbonyl carbon and the amide nitrogen. Due to this planarity,

dx.doi.org/10.1021/jo3003776 | J. Org. Chem. 2012, 77, 4968–4979

Table 1. Observed and Calculated NMR Chemical Shifts and Coupling Constants for the Ring Hydrogen Atoms of 6a, 6c, and 7c[a]

compd	H_{cis} (ppm)	H_{trans} (ppm)	$\Delta\nu$ (trans−cis) (ppm)	$^2J_{HH}$ (Hz)	$^3J_{PH}$(cis) (Hz)	$^3J_{PH}$(trans) (Hz)
6a (obs)	3.53				3.7	
6a (DFT)	3.46				3.4	
6c (obs, −40 °C)	3.864	3.936	0.072	17.5	3.8	−1
6c (obs, +50 °C)	3.835	3.840	0.005			
6c$_1$ (DFT)	3.87	4.42	0.56	−16.8 (−19.4[b])	3.7 (4.1[b])	−3.1 (−3.0[b])
6c$_2$ (DFT)	3.87	3.84	−0.03	−18.0 (−20.6[b])	2.7 (3.6[b])	−2.2 (−2.0[b])
syn-**6c** (DFT)	4.46	3.89	−0.57	−15.9	3.8	−3.7
7c (obs, −30 °C) major	4.29	4.02	−0.27	18.0	6.2	1.45[c]
7c (obs, −30 °C) minor	4.24	4.02	−0.22	18.0	5.9	1.45[c]
7c (DFT)	4.42	4.45	0.02	−18.0 (−20.8[b])	5.8 (6.5[b])	−3.2 (−3.0[b])
E-**7c**$_1$ (DFT)	4.34	4.49	0.15	−17.5	6.0	−3.5
E-**7c**$_2$ (DFT)	4.15	3.83	−0.33	−17.7	7.0	−2.7

[a]Calculations for **6a** did not include solvation, whereas those for **6c**, *syn*-**6c**, **7c**, and *E*-**7c** used PCM with $CHCl_3$ solvation. [b]Calculated using the uncontracted 1s orbitals; see below. [c]Observed averaged $^3J_{PH}$(trans) at 60 °C for **7c**; the peaks were too broad to resolve coupling at −30 °C.

the PNCH and PNCC(isopropyl) dihedral angles (−118.7° and 119.9°, respectively) are nearly equal albeit opposite; for the purposes of this paper, since the sign of the dihedral angle is relevant, all values are reported for the S_P configuration, i.e., that shown for **6** in Figure 2, so these dihedral angles are the opposite of those that would be given by the known R_P configuration shown for **7a** in Figure 2. On the basis of a "normal" Karplus equation, then, one would predict equal vicinal phosphorus−hydrogen coupling constants in **7c**. Instead, for the cis-hydrogen (see Figure 2 for cis/trans definitions[35]), $^3J_{PH}$ = 6.2 Hz, and for the trans-hydrogen, $^3J_{PH}$ = 1.45 Hz (using average values for the major and minor *t*-Boc rotamers[35]). These values are comparable to those seen in our closely related *N*-toluenesulfonyl-1,3,2-oxazaphospholidines **6a**,**b**, even though the nitrogen is pyramidal in the latter compounds rather than planar as in the *N*-Boc derivatives, allowing the cis and trans dihedral angles to be different.

In order to check the dihedral angles and coupling constants, the structures and NMR spectra of **7b** and **7c** were calculated using *Gaussian 03* and *09*;[48] the alanine analogue **7b** was examined rather than **7a** in order to avoid unnecessary complications due to isopropyl rotation. Following published recommended levels of theory,[49−51] DFT energy optimization was carried out (B3LYP, 6-31G(d) basis set), including a frequency calculation to ensure that a true local minimum was found, followed by a single-point DFT energy and NMR calculation (B3LYP, GIAO, 6-311+G(2d,p) basis set). Similar methods have been reported for $^3J_{PH}$, mostly for phosphine oxides and sulfides.[52] The calculations for **7b** and **7c** were carried out using the default polarizable continuum model (PCM) for solvation by $CHCl_3$ in order to more accurately model conformational energies (see below), but the structural and NMR values were little changed by the PCM calculation. More recently, recommendations for calculation of high-accuracy one- and two-bond coupling constants have been published,[53] and these methods will be considered after all of our examples have been introduced. Selected X-ray (**7a**) and calculated (**7b**,**c**) structural data may be found in the Supporting Information, and NMR data may be found in Table 1.

Just as with the X-ray structure of **7a**, the calculated **7b**,**c** heterocycle rings were essentially planar, the relevant PNCH or PNCC dihedral angles were nearly identical, and the amide was found to adopt the *Z t*-Boc conformation;[35,44] the overall bond lengths and angles were very similar to those seen in the X-ray structure of **7a**. Further support for the assumption that the *Z t*-Boc conformation was the major isomer in solution[35] was provided by optimizing the *E t*-Boc conformation of **7b** and of **7c**, which located a secondary minimum that was 0.40 kcal/mol higher in energy for **7b** and two minima that were 0.33 (*E*-**7c**$_1$) and 1.06 (*E*-**7c**$_2$) kcal/mol higher for **7c**; these energy differences would give 30% of the minor isomer of **7b** at −40 °C and 38% of the minor isomer of **7c** at −30 °C, with observed values of 14% and 19%, respectively. Given the small energy differences, the agreement is reasonable. The calculated coupling constants for **7c** (Table 1), $^3J_{PH}$(cis) = 5.8 Hz and $^2J_{HH}$ = −18.0 Hz, were in excellent agreement with those observed (6.2, 18.0 Hz, respectively), while $^3J_{PH}$(trans) = −3.2 Hz was qualitatively in agreement with the observed value of ∼1.5 Hz and of course suggested that it is in fact negative. While the simplest assumption is that the major isomer of **7c** is still the *Z t*-Boc conformation, neither the calculated chemical shifts nor the calculated coupling constants distinguish between the conformations. The coupling constants for both the *Z* and *E* conformations were similar (Table 1), so at least the conclusion that $^3J_{PH}$(trans) is negative is not affected. The calculated chemical shifts for the two major conformations (*Z*-**7c**, *E*-**7c**$_1$) are close to those observed for H_{cis}, but the calculated values for H_{trans} are ∼0.5 ppm downfield from those observed. In contrast the minor *E* conformer *E*-**7c**$_2$ gave calculated chemical shifts in good agreement with those observed (4.15 and 3.82 ppm for H_{cis} and H_{trans}). It differs most notably from the other conformers by a ∼80° rotation of the phenyl group, which is nearly lined up with the P−N bond in each of *Z*-**7c**, *E*-**7c**$_1$, and even the X-ray structure of **7a**, with NPCC dihedral angles of −21.0°, −29.0°, and −30.4°, respectively; in the higher energy conformer *E*-**7c**$_2$, the NPCC dihedral angle is −101.2° and the OPCC dihedral angle is −9.8°, so the phenyl nearly eclipses the P−O bond (see Table S-2 in the Supporting Information for details). Clearly the chemical shift positions are sensitive to the phenyl ring conformation, and at the NMR temperatures, there is more than enough thermal energy to give rise to a range of conformations that makes such fine distinctions in calculations of these chemical shifts difficult.

***N*-Toluenesulfonyl Heterocycles.** The X-ray crystal structure of the *N*-toluenesulfonylvaline-derived heterocycle **6a** has been described in detail;[36] it exhibits an envelope

dx.doi.org/10.1021/jo3003776 | J. Org. Chem. 2012, 77, 4968−4979

conformation and non-identical PNCH and PNCC(isopropyl) dihedral angles of 139.0° and −98.4°. Optimization of this structure as described above but without the PCM calculation again gave a similar structure, with for instance very similar dihedral angles of 135.0° and −102.8°. The calculated coupling constant (Table 1) $^3J_{PH}$(cis) = 3.4 Hz was similarly in excellent agreement with that observed (3.7 Hz).

In order to complete the cis/trans analysis in the manner seen for glycine derivative **7c**, even though it was not strictly required since both cis and trans isomers of **6a,b** were observed, the synthesis of the glycine-derived *N*-toluenesulfonyl heterocycle was carried out. Reaction of *N*-*p*-toluenesulfonylglycine with $PhPCl_2$ occurred immediately to give **6c** (eq 2), but

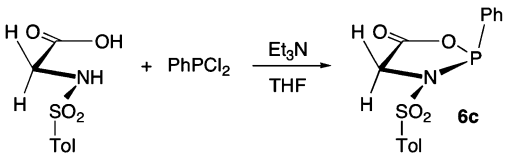

(2)

purification was accomplished only with surprising difficulty due to persistent contamination by the $Et_3NH^+Cl^-$ byproduct and an unidentified brown impurity. In the absence of any compelling reason to optimize the synthesis, and because the procedure was reproducible (albeit in 6% yield), we have abandoned further attempts to purify **6c** in high yield. Details may be found in the Experimental Section.

The ^{1}H NMR spectrum of **6c** taken at room temperature could not be readily interpreted, so spectra were taken from −40 to +50 °C (Figure 3). At temperatures from −40 to 0 °C,

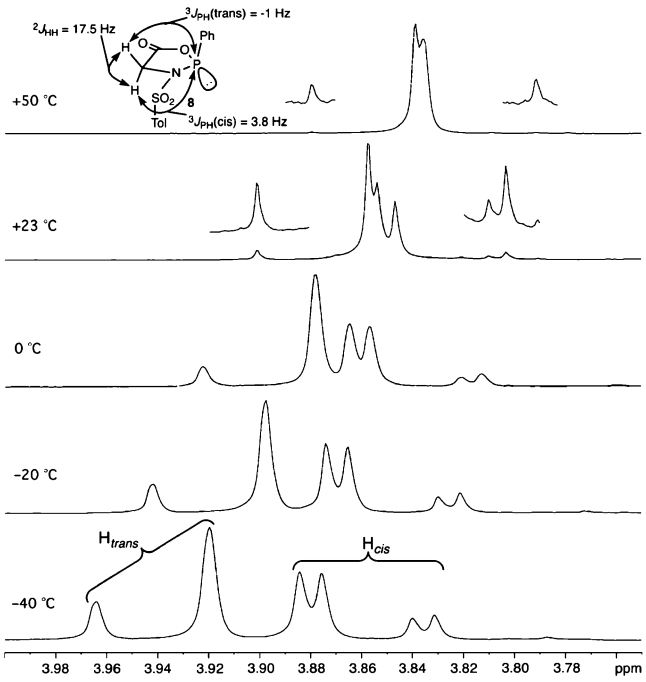

Figure 3. Variable temperature ^{1}H NMR spectra of **6c** in $CDCl_3$.

the observed doublet of doublets and doublet for the cis and trans hydrogens, respectively, would arise from a straightforward fit of chemical shifts and coupling constants, namely, a large geminal coupling constant $^2J_{HH}$ = 17.5 Hz, and typical phosphorus−hydrogen coupling constants for the cis and trans hydrogen atoms ($^3J_{PH}$(cis) = 3.8 Hz, compared to 3.7 and 3.4 Hz in *cis*-**6a,b**; $^3J_{PH}$(trans) = 0 Hz compared to 1.4 Hz in *trans*-**6a,b**).[36] The chemical shifts were clearly temperature-dependent, with the trans-hydrogen in particular moving upfield by ∼30 Hz (0.08 ppm) from −40 °C to +23 °C. At room temperature, however, the chemical shift difference of the geminal protons is less than their coupling constant (i.e., ($\Delta\nu_{HH}/J_{HH}$ = 0.6), and simulation of the ABX spectrum using the above coupling constants (in particular $^3J_{PH}$(trans) = 0 Hz) showed that virtual coupling would necessarily result in *both* hydrogen atoms giving rise to a doublet of doublets.

The problem was solved by experimentation with small negative coupling constants for one of the vicinal phosphorus−hydrogen coupling constants; while ABX spectra allow only the relative signs of J_{AX} and J_{BX} to be determined, it is more likely here that the larger $^3J_{PH}$(cis) will be positive. In fact, the three lowest-temperature spectra were readily fit with $^3J_{PH}$(trans) = 0 to −1.2 Hz, whereas that at 23 °C was fit with $^3J_{PH}$(trans) = −0.7 to −2.1 Hz. All four spectra gave excellent fits using $^3J_{PH}$(trans) = −1 Hz. At 50 °C, these coupling constants also gave an excellent fit of the calculated and observed spectra.

In order to check values and signs of the derived coupling constants, DFT calculations were run on **6c** as described above for **7**. The initial coordinates were taken from the X-ray crystal structure of **6a** and allowed location of a local minimum with a similar structure (**6c$_2$**); however, as seen for *E*-**7c**, a phenyl conformer (**6c$_1$**) that was lower by 0.2 kcal/mol was also located. The overall bond lengths and angles were very similar to those seen in the X-ray and DFT structures of **6a**, and the phenyl in **6c$_1$** was rotated ∼60° from that in both **6a** and **6c$_2$**, very nearly eclipsing the P−N bond.

The temperature-dependence of the ABX system suggested to us that it might be caused by rotation of the tolyl moiety about the sulfonamide S−N bond. The B3LYP/6-31G(d) optimized structure was used as a starting point, in which, following rotation about the S−N bond by both 160° and 180°, the structure was reoptimized. The geometry converged to the same structure, namely a syn conformation (*syn*-**6c**) that was 0.8 kcal/mol higher in energy than the anti conformation of **6c$_2$**. The phenyl was rotated a further ∼20° from the conformation seen in **6c$_1$**, ∼80° from that seen in both the X-ray structure and **6c$_2$** and again close to eclipsing the P−N bond. Because of the methylene chemical shift sensitivity to phenyl conformation seen for **7c**, other minima were sought, but none were found. Other than the phenyl conformation, overall bond lengths and angles were again similar as described above (see Table S-2 in the Supporting Information for details).

Chemical shifts and coupling constants were calculated at the B3LYP/6-311+G(2d,p) level (Table 1). Just as seen for **7c**, the calculated coupling constants for **6c$_1$**, **6c$_2$**, and even *syn*-**6c** were in agreement with those observed (Table 1). Unlike the example for **7c**, however, here the calculated signs of the cis and trans coupling constants *confirm* the experimental determination that $^3J_{PH}$(cis) and $^3J_{PH}$(trans) have opposite signs and of course suggest that $^3J_{PH}$(trans) is negative. Experimental determination of the absolute signs of these coupling constants is not trivial and will be reported in due course, but preliminary results using e.cosy directly confirm (without resorting to the ABX simulation) that the two vicinal coupling constants have opposite signs.[54]

The NMR chemical shifts were calculated as described above (Table 1) and, similar to those seen for **7c**, are only roughly in agreement with those observed. The calculated difference between the chemical shifts of the trans and cis hydrogen atoms

dx.doi.org/10.1021/jo3003776 | J. Org. Chem. 2012, 77, 4968−4979

is −0.03 ppm in **6c**$_2$, virtually the same as the observed 0.07 and 0.005 ppm differences at −40 and 50 °C, but is 0.6 ppm in **6c**$_1$ and −0.6 ppm in *syn*-**6c**, so like **7c** the chemical shift positions are sensitive to phenyl conformation. These results will be revisited in the Discussion section.

Me_2NPCl_2 (2) and *t*-$BuPCl_2$ (3). Given the overall success of the DFT calculations for **6c** and **7c**, coupling constants were calculated for **2** and **3** since experimental data were similarly available for comparison as shown in Figure 1. Each of **2** and **3** was optimized (B3LYP/6-31G(d)) and coupling constants were calculated (6-311+G(2d,p)) as before. Due to the presence of the third-row chlorine atoms, the optimization was checked using a slightly higher level basis set, 6-31+G(d,p), but scarcely any difference in geometry or coupling constants was seen, thereby justifying the use of the smaller basis set for optimization. The results are shown in Figure 4, and selected

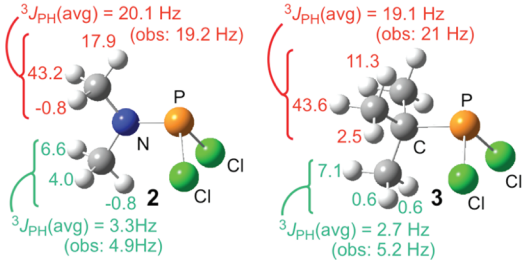

Figure 4. Calculated and observed vicinal P−H coupling constants in **2** and **3** (shown at each hydrogen atom, in Hz); values are shown for only one of the two symmetry-related methyl groups in **3**.

structural data may be found in the Supporting Information. The coupling constants for the hydrogen atoms on the methyl groups gauche and anti to the phosphorus lone pair were calculated as the average of the three static values, and these values could then be compared to the reported observed values. As seen in Figure 4, the agreement between the calculated and observed values is quite good for the larger values for the hydrogen atoms on the gauche methyl groups, similar to the agreement for the larger cis values for **6c** and **7c**, but poorer for the smaller values for those on the anti methyl groups, again just as seen for the smaller trans values for **6c** and **7c**.

CH_3OPH_2. Since both the experimental data and the DFT NMR calculations described above were inconsistent with a simple dependence of vicinal phosphorus−hydrogen coupling constant on dihedral angle, a more systematic analysis was carried out. The simplest system, that is, one consisting of the fewest number of atoms and electrons, that could be used to reasonably test the dependence of $^3J_{PH}$ on both the P−H dihedral angle and phosphorus lone pair conformation is arguably CH_3OPH_2; any other intervening atom between the methyl group and phosphorus would require additional atoms. As defined in Figure 1 and shown here in Figure 5, the dihedral angle θ was allowed to vary from 0 to 100° in 20° increments, and one of the hydrogen−phosphorus−oxygen−carbon dihedral angles ω' was driven from 0 to 360° in 15° increments. The structure was then optimized (DFT, B3LYP) at the 6-31G(d) level but with the two dihedral angles θ and ω' held constant. For each point, three POCH dihedral angles were thereby generated (and three values of $^3J_{PH}$); while only one of the POCH dihedral angles was constrained as described above, the other two were very close to 120° and 240° apart, allowing the entire 360° of rotation to be calculated. Following each

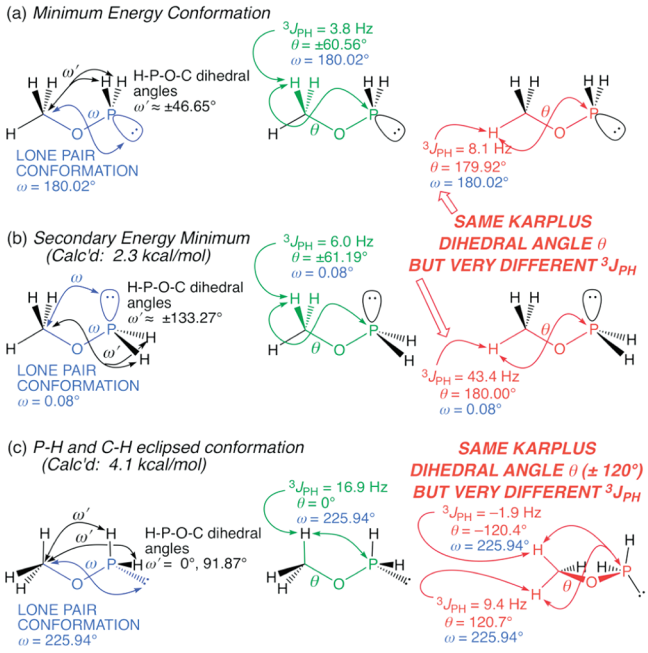

Figure 5. Representative structures showing $^3J_{PH}$ as a function of POCH and lone pair conformation in CH_3OPH_2.

constrained optimization, the NMR coupling constants were calculated (DFT, B3LYP) at the 6-311+G(2d,p) level. For presentation of the data, we have found it preferable to use the putative lone pair-carbon dihedral angle ω rather than ω', which was calculated by adding 180° to the average of the two HPOC dihedral angles. Coupling constants are shown in Figure 5a, b, and c, respectively, at the global energy minimum, a local minimum (2.3 kcal/mol), and a higher energy structure (4.1 kcal/mol) that would correspond to a planar ring if the eclipsed hydrogen atoms were joined; the global maximum (5.5 kcal/mol) occurs near a further 30° rotation (ω = 256.2° = −103.8° and ~symmetrically at 106.4°). The full surfaces of 475 points for θ,ω = 0−360° were generated for each of $^3J_{PH}$ and relative energy (Figure 6). As seen in Figure 6a,b, due to the lone pair $^3J_{PH}$ has only 2-fold symmetry with respect to both θ (albeit only approximately) and ω, while the energy has 3-fold symmetry with respect to methyl rotation (that is, for θ), but 2-fold symmetry with respect to PH_2 rotation (that is, for ω). Overall, the vicinal coupling constants range from −2.7 Hz (at $\theta,\omega \approx$ 120°, 120° and at −120°, −120°) to 43.4 Hz (at θ,ω = 180.0°, 0.1°). This latter point was not taken from those calculated at 15° increments from ω', but instead the value ω' = 133.35° was chosen since based on the average HPOC dihedral angles in other structures, it was expected to give a value of ω close to zero. The angular dependences are consistent with those seen in Figures 1 and 2 and will be analyzed in the Discussion section.

$(CH_3)_2NPH_2$ and $(CH_3)_3CPH_2$. Given the calculated results for CH_3OPH_2, where for instance for θ = 180°, $^3J_{PH}$ ranges from 8.1 Hz (at ω = 180°) to 43.4 Hz (at ω = 0°), it seemed important to check that the result was independent of the intervening atoms. In a similar manner as described above, coupling constants were calculated for one of the methyl groups bound to N and C in dimethylaminophosphine and in *tert*-butylphosphine. Plots of $^3J_{PH}$ versus the dihedral angles θ and ω are similar to that seen in Figure 6a for CH_3OPH_2 (see Supporting Information for details); for $(CH_3)_2NPH_2$, $^3J_{PNCH}$

dx.doi.org/10.1021/jo3003776 | J. Org. Chem. 2012, 77, 4968−4979

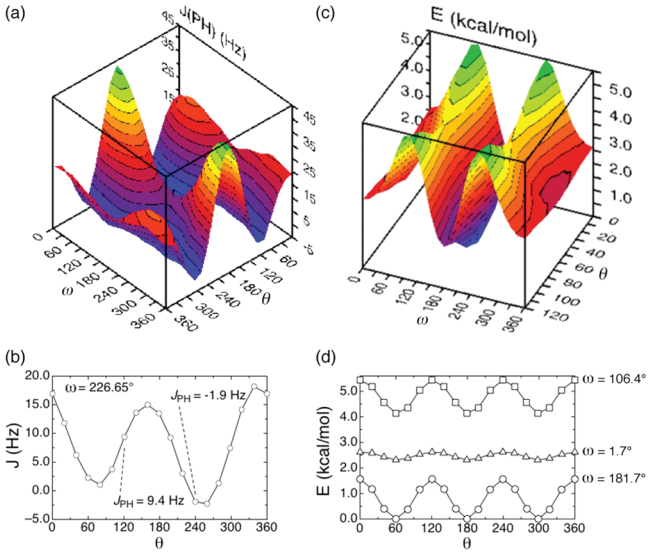

Figure 6. (a) Plot of $^3J_{PH}$ (Hz) versus dihedral angles θ and ω (deg) calculated for CH_3OPH_2. (b) 2D plot of a "slice" of 3D graph from part (a), for ω = 225.9°, corresponding to the structure in Figure 5c at θ = 0°, 120°, and 240° (i.e., −120°). (c) Plot of relative conformational energy versus θ (the surface is identical for θ = 120°−240° and 240°−360°) and ω. (d) 2D plots of "slices" of 3D graph from part (c), for $\omega \approx 0°$, 106.4°, and ∼180°, slices that include the structure shown in Figure 5b (a local minimum), the global maximum, and the structure shown in Figure 5a (the global minimum), respectively.

ranged from −4.4 Hz (at θ,ω = 120°, 120° and at −120°, −120°) to 49 Hz (at θ,ω = 180°, 30°), and at the same Karplus angle θ = 180°, $^3J_{PH}$ = 2.8 Hz at ω = 180°. For $(CH_3)_3CPH_2$, $^3J_{PCCH}$ ranged from −1.2 Hz (at θ,ω = 80°, 120°; 80°, 150°; −80°, −120°; −80°, −150°) to 51 Hz (at θ,ω = 180°, 0°), but in a similar manner to that noted above, at the same Karplus angle θ = 180°, $^3J_{PH}$ = 0.5 Hz at ω = 180°.

Basis Set Comparisons. As described at the outset of the Results section, NMR calculations at the 6-311+G(2d,p) level have been considered reliable. However, recent work, particularly with calculations of one and two-bond coupling constants, has suggested a need for refinements aimed at better modeling the electron density close to the nucleus, including uncontracting the basis set and addition as needed of tight s, p, and d orbitals.[53,55] Results of NMR calculations using a variety of basis sets on CH_3OPH_2 (optimized by DFT with the B3LYP functional at the 6-31G(d) level) are collected in Table 2. The uTZ-w basis set is strongly recommended by Deng, Cheeseman, and Frisch because it gives spin−spin coupling constant results that are close to the basis set limit.[53] It is interesting therefore that the 6-311+G(2d,p) basis set gave values that were only 7−9% lower, at a far lower computational cost, and the uncontracted version of this basis set with additional tight s functions gave values that were nearly indistinguishable from those using the uTZ-w set, i.e., within 0.3 Hz. The much larger aug-ccPVDZ and aug-cc-PVTZ basis sets were much worse, and this has been noted before for one- and two-bond coupling constants.[53]

Three additional examples were calculated, namely, **6c$_1$**, **6c$_2$**, and **7c**, and the results are shown in Table 1. Using a total of 1120 and 1004 basis functions, respectively, the u6-311G-w basis set gave slightly better values for $^3J_{PH}$ but slightly worse for $^2J_{HH}$ than those using the smaller 6-311+G(2d,p) basis set of 694 and 617 functions, respectively.

DISCUSSION

The coupling constant data for planar *t*-Boc heterocycle **7** provides the simplest unambiguous example that a Karplus-type equation predicting $^3J_{PH}$ on the basis of P−H dihedral angle is insufficient for trivalent phosphorus. That is, in **7a**, the two PNCH and PNCC(isopropyl) dihedral angles from the X-ray crystal structure are −118.7° and 119.9° while the corresponding calculated PNCH angles for glycine analogue **7c** are virtually the same at −119.1° and 119.8°, yet the observed $^3J_{PH}$ coupling constants are 6.2 and 1.45 Hz for the cis and trans hydrogen atoms. A DFT calculation of these coupling constants provided theoretical confirmation of this difference, giving $^3J_{PH}$ = 5.8 Hz for the cis hydrogen and −3.2 Hz for the trans hydrogen, and 6.5 and −3.0 Hz using the larger and presumably more accurate u6-311+G(2d,p)-w basis set;[53] that is, on the basis of the calculation, the smaller value was in fact negative.

The variable temperature NMR spectra of *N*-sulfonyl heterocycle **6c** provided direct experimental evidence that the trans coupling constant was indeed negative. The spectra shown in Figure 3 are serendipitous in the sense that due to the non-first-order system, the only way that the simulated ABX spectra could be fit to the observed spectra was to assign unlike signs to the vicinal coupling constants, giving $^3J_{PH}$ = 3.8 Hz for the cis hydrogen and −1 Hz for the trans hydrogen if the larger value is assumed to be positive. Here too, the DFT calculations were in accord, giving values of 3.7, 2.7 Hz and −3.1, −2.2 Hz, for **6c$_1$** and **6c$_2$**, respectively, using the 6-311+G(2d,p) basis set, and 4.1, 3.6 Hz and −3.0, −2.0 Hz using the u6-311+G(2d,p)-w basis set. Clearly for both **6c** and **7c** there is no compelling reason to use the larger basis set, so while the results are imperfect they are qualitatively sufficient. Together with the basis set comparison shown in Table 3 the use of the 6-

Table 2. Calculated CH_3OP Coupling Constants (Hz) for CH_3OPH_2 (ω = 0.1°, θ = 180, ±61.2°) Using Different Basis Sets

basis set[a]	no. basis functions	$^3J_{PH(anti)}$	$^3J_{PH(gauche)}$	$^2J_{HH(ag)}$	$^2J_{HH(gg)}$	*E* (au)
6-31G(d)	59	38.46	5.21	−13.05	−10.18	−457.66667262
u6-31G-w	154	46.21	5.99	−12.83	−9.39	−457.66666944
6-311+G(2d,p)	119	43.45	6.05	−11.41	−8.47	−457.74525041
u6-311G-w	200	47.56	6.39	−12.49	−9.36	−457.74524208
aug-cc-pVDZ	118	39.14	5.85	−10.98	−8.39	−457.70508336
uDZ-w	244	47.51	6.43	−12.25	−9.13	−457.70507807
aug-cc-pVTZ	257	39.49	5.98	−9.53	−6.74	−457.75990772
uTZ-w	389	47.82	6.46	−12.25	−9.16	−457.75990187

[a]See ref 53 for basis set abbreviations; briefly, u is the uncontracted basis set, w indicates the incorporation of additional s functions, and each of the u,w basis sets uses the preceding basis set in the table as its starting point. See Experimental Section for further details.

dx.doi.org/10.1021/jo3003776 | J. Org. Chem. 2012, 77, 4968−4979

311+G(2d,p) basis set as the minimal basis set for these systems is justified, and our conclusion that a modest basis set can suffice for 3-bond coupling is not without precedent.[51]

Just as both the X-ray structure of **7a** and the calculated low energy conformations of **7b** and **7c** exhibited the *Z*-*t*-Boc conformation, the X-ray structure of **6a** and the low energy conformations of **6c** each exhibited the *anti*-tolyl conformation (Figure 7). Once again the simplest assumption would be that

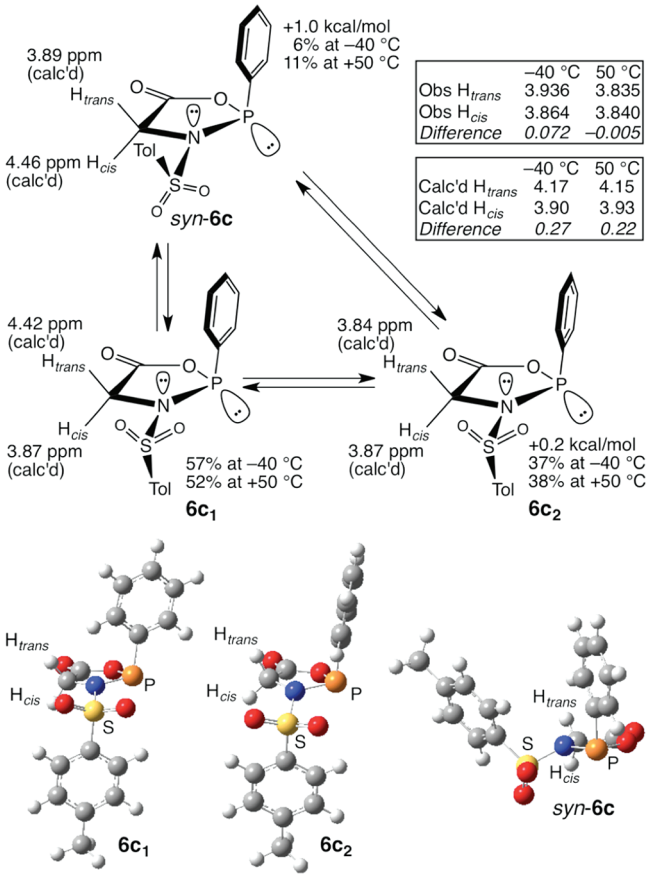

Figure 7. NMR chemical shifts and calculated structures for equilibrating N–S rotamers **6c**$_1$, **6c**$_2$, and *syn*-**6c**; for clarity the view of *syn*-**6c** has the phosphorus atom in front and allows one to view the pyramidalization at nitrogen and the PNCH dihedral angles.

the conformers observed in solution are the lower-energy anti conformers (**6c**$_1$, **6c**$_2$), and so the possibility was investigated that equilibration with the syn conformer might provide an explanation for the observed temperature dependence of the chemical shifts; while not directly related to the theme of this paper, it is relevant since it is related to the experimental evidence of the signs of the P–H vicinal coupling constants. We have previously surveyed and discussed sulfonamide geometry,[36] in which theoretical work[56−58] has shown that there is a 2-fold torsional barrier to rotation about the sulfur–nitrogen bond with a minimum for the eclipsed conformation represented by *syn*-**6c** and a secondary minimum for the staggered conformations represented by **6c**$_1$ and **6c**$_2$ (eclipsed and staggered since both N and S are pyramidal/tetrahedral as seen in Figure 7). The reason for the calculated preference for *anti*-**6c** despite its staggered conformation is unknown, and even the nominally eclipsed *syn*-**6c** is rotated ~30° past the eclipsed conformation. The calculated chemical shifts for the conformers support **6c**$_1$ and **6c**$_2$ as the predominant conformers because the observed methylene proton chemical shifts are nearly coincident as are those calculated for **6c**$_2$, which would be averaged with those for **6c**$_1$ (which are separated by 0.55 ppm but position H_{cis} upfield of H_{trans} as is observed); the chemical shifts for *syn*-**6c** are separated by nearly 0.6 ppm and in the opposite direction. The calculated energy differences of the conformers allows the temperature dependence of their concentrations to be estimated, with a predicted increase in concentration of *syn*-**6c** from 6% to 11% of the mixture on going from −40 to +50 °C. Qualitatively this would lead to a shrinking of the chemical shift difference between the methylene protons, and while they are much closer than calculated (see Figure 7 for observed and calculated chemical shifts), the predicted *change* on heating is virtually the same as that observed. As noted for **7c** and as seen here for **6c**$_1$ and **6c**$_2$, these chemical shifts are clearly sensitive to the phenyl ring conformation, and so the optimized geometries alone do not provide a particularly precise set of chemical shifts. The *cause* of both the large downfield shift of the cis hydrogen and the upfield shift of the trans hydrogen in *syn*-**6c** might be supposed to be due to aromatic ring anisotropy, with H_{trans} in the shielding cone and H_{cis} in the deshielding region of the tolyl, so a calculation of the chemical shifts for the *methane*sulfonamide (i.e., with a methyl group in place of the tolyl moiety) was carried out. The chemical shift of H_{trans} increased to 4.34 ppm, so the upfield shift due to shielding by the toluenesulfonyl moiety seems to be a reasonable supposition, but the chemical shift of H_{cis} was (at 4.47 ppm) virtually unchanged. An alternative explanation for the downfield shift from both **6c**$_1$ and **6c**$_2$ to *syn*-**6c** might be that it arises due to proximity of an S–O bond to H_{cis}, but given the sensitivity to phenyl ring conformation, further speculation is unwarranted.

Given the sensitivity of the chemical shifts of H_{cis} and H_{trans} to phenyl ring conformation, it seemed appropriate to investigate whether the coupling constants might exhibit any changes as well. In particular, since $^3J_{PH}$ is dependent on the lone pair-carbon dihedral angle ω, any significant interactions of the phenyl π-system with the phosphorus lone pair, as has been documented for the nitrogen analogue aniline,[59,60] might alter $^3J_{PH}$. While some interaction might be possible in phosphines, with the apparent exception of vinylphosphine where the most stable structure appears to arise due to π-lone pair overlap,[61] the effect is small for the more diffuse phosphorus lone pair compared to that of nitrogen.[59,62,63] Examination of Figure 7 suggests that the phenyl rings in **6c**$_1$ and **6c**$_2$ are orthogonal to each other, with the phenyl approximately eclipsing the putative lone pair (and hence minimizing any π-interaction) in **6c**$_1$, and approximately lying orthogonal to the lone pair (and hence maximizing any π-interaction) in **6c**$_2$. The coupling constants differ by ~1 Hz (Table 1), but interpretation of whether this is consistent or not with differing π-interactions is complicated by the facts that both are optimized structures and so have different PNCH dihedral angles, and the phenyl ring geometries relative to the lone pair are only approximately as described. In order to better answer this question, calculation of $^3J_{PH}$ following rotation of the phenyl group in **6c**$_1$ to the position where it would bisect the NPO angle (i.e., $\angle(OPCC_{Ph} = NPCC_{Ph} = \pm 45.9°)$ or be orthogonal (i.e., $\angle(NPCC_{Ph} = -135.9°)$ but leaving all other parameters unchanged (and giving models that still look very similar to those in Figure 7), was carried out. The trans coupling constant of −3.1 Hz remained relatively unchanged, while the cis coupling constant of 3.7 Hz changed slightly in

dx.doi.org/10.1021/jo3003776 | J. Org. Chem. 2012, 77, 4968–4979

both directions: for $\angle(\mathrm{NPCC_{Ph}}) = -45.9°$, $^3J_{PH}$(cis) and $^3J_{PH}$(trans) = 3.0 and −3.6 Hz respectively, while for $\angle(\mathrm{NPCC_{Ph}}) = -135.9°$ $^3J_{PH}$(cis) and $^3J_{PH}$(trans) = 4.5 and −3.3 Hz, respectively. The values indicate that phenyl conformation does have a small effect on the vicinal phosphorus hydrogen coupling constants, but not in any clear manner and not enough to affect any of our conclusions.

A final point concerns the presumed position of the lone pair whose overlap with the phenyl ring was considered for its effect on the coupling constant. As described above for CH_3OPH_2, the putative lone pair-carbon dihedral angle was calculated by adding 180° to the average of the two HPOC dihedral angles, and the same was done here by using the average of the CNPO and $\mathrm{CNPC_{Ph}}$ dihedral angles; values are collected in Supporting Information Table S-2. For **6c$_1$**, the calculated lone pair position was coplanar with the phenyl ring when it bisected the NPO angle as described above (within ∼1°; further precision is not possible because the DFT calculation does not give a perfectly planar phenyl ring), and therefore also necessarily orthogonal to the phenyl ring when it was rotated 90°. In an effort to determine if this calculation provides a valid determination of the lone pair position, the X-ray structures of two phosphorus heterocycles that are analogues of **6** and **7** were examined,[64] in which each has a BH_3 moiety bound to phosphorus; in this way, the calculated "lone pair" position can be compared to the actual position of the boron atom. One heterocycle was derived from (−)-ephedrine, and the other from *S*-1,1-diphenyl-1,2-propanediol, and the calculated lone pair dihedral angles all agreed with the CNPB and COPB dihedral angles to within 3.5° or better (see Figure S-2, Supporting Information). We conclude that the use of these dihedral angles to approximate the lone pair position is reasonable.

One of the motivations for the synthesis of glycine derivatives **6c** and **7c** was that if phosphorus inversion was sufficiently rapid, the two ring hydrogen NMR signals should undergo coalescence. As shown above, the chemical shift coalescence in **6c** is readily accounted for by sulfonamide rotation, not phosphorus inversion. Just as a lower limit for the barrier for phosphorus inversion in **7c** of 21 kcal/mol was determined,[35] there is also no evidence that inversion is occurring in **6c**. At 23 °C, the rate of exchange must be less than ∼0.2 s^{-1} since at that rate broadening of the peaks at the "wings" of the multiplet in Figure 3 would be evident. The spectrum at 50 °C is broader, and here the simulation of inversion does not give a worse fit. The rate constant at 23 °C translates into an inversion barrier of greater than 18 kcal/mol, a number that is likely to be significantly lower than the true barrier, since measured barriers for phosphine inversion[65] are 29−36 kcal mol^{-1} and for phosphite inversion[66] ∼33 kcal mol^{-1}.

The low temperature NMR spectra of **2** and **3** for which data are given in Figure 4 are remarkable for several reasons. The agreement between the observed and calculated coupling constants first of all confirms that the interpretations by the Cowley,[23] Roberts,[25] and Bushweller[26] groups of the 60 MHz variable temperature NMR spectra recorded some 40 years ago were correct. The anomalously high coupling constants of 19−21 Hz were also in accord with those being reported at that time by the Gagnaire[22,24] and Bentrude[27] groups. However, most of these are *averaged* coupling constants.[23−26] As seen in Figure 4, for instance, these averages are well-matched by the DFT calculations, as are the requirements for unusually large $^3J_{PH}$ values noted for Figure 1: that is, for the conformations in which the phosphorus lone pair is gauche to the CH carbon atom, the anti hydrogen atoms (with PYCH dihedral angles of 180°) have calculated vicinal PH coupling constants over 40 Hz, values that have not been observed directly in such systems. The low temperature NMR spectra of **2** and **3** provide, in conjunction with the DFT calculations, experimental evidence of the validity of these 40 Hz coupling constants.

The calculation of coupling constants for CH_3OPH_2 yields a three-dimensional curve giving $^3J_{PH}$ as a function of the two angles θ and ω. We started off this paper with an account of the Karplus equation, so in principle a two-dimensional Karplus equation could be fit as a function of θ and ω to the theoretical data. In practice, we have found that such a modified Karplus equation is not a useful construct. For instance, in keeping with tradition, we tried a cosine (and sin) type of function and found that simple extensions could give at best qualitative fits to the observed surface shown in Figure 6a, while failing to be of any quantitative use. As one example, a 15-parameter fit that included all possible terms up to fourth-order (i.e., including $A_n \cos^a\theta \cos^b\omega$ ($a + b = 4, 3, 2, 1, 0$ for $a,b \geq 0$, A_n = best-fit parameter, $n = 1-15$) gave a 2-fold symmetrical surface (with respect to θ and ω) and a standard deviation in $^3J_{PH}$ of 3.0 Hz, but this average masked the details. The poor fit arises because the DFT-calculated surface is *not* symmetrical with respect to $\theta = 180°$. That is, the local maxima in $^3J_{PH}$ along the central "ridge" in Figure 6a go from $\theta = 180°$ to 200°, back to 180°, then to 160°, and then return to 180° as ω increases from 0° to 360°; the effect is easily seen by plotting some ω slices for $\omega =$ 0°, 120°, 180°, and 240° (Figure S-3, Supporting Information; see also Figure 6b) but is not readily visible by inspection of Figure 6a.

A modified two-dimensional 8 to 10-parameter Karplus equation was eventually devised in which the traditional Karplus coefficients and torsional angle θ were themselves sine and cosine functions of the lone pair angle ω (eq 3);

$$
\begin{aligned}
^3J_{PH} = {} & A_1 \cos^2(\theta + \theta_c + \alpha) - B_1 \cos(\theta + \theta_c + \alpha) + C_1 \\
A_1 = {} & A_2 \cos^2(\omega + \omega_c) - B_2 \cos(\omega + \omega_c) + C_2 \\
B_1 = {} & A'_2 \cos^2(\omega + \omega_c) - B'_2 \cos(\omega + \omega_c) + C'_2 \\
\alpha = {} & D \sin(\omega + \omega_c)
\end{aligned}
\qquad (3)
$$

details of the derivation, parameter values, andfit to the DFT results may be found in the Supporting Information. While the form of this equation might have some utility in special cases if one had large amounts of data for a specific system, in practice this is not a practical means for accurate calculation of vicinal P−H coupling constants, and not just because of the complexity of eq 3. First, different parameter sets are needed for the three cases we examined; that is, for $^3J_{PYCH}$, three sets of parameters are needed to provide adequate fits for each of Y = O, N, C. For the nitrogen case the fit was particularly poor, because the pyramidalization at nitrogen changed in irregular fashion as θ and ω were changed, leading to a somewhat "noisy" calculated surface, and even so, two additional parameters (the constants θ_c and ω_c) were necessary to give a good fit. For CH_3OPH_2, there was no improvement in the fit when these two parameters were included (that is, $\theta_c \approx \omega_c \approx 0$), but for $(CH_3)_3CPH_2$, not just $\theta_c = \omega_c = 0$, but even $D \approx 0$,

dx.doi.org/10.1021/jo3003776 | J. Org. Chem. 2012, 77, 4968−4979

so $^3J_{PCCH}$ was virtually symmetrical about θ = 180°. The interesting conclusion from this is that the non-zero values of α seen in CH_3OPH_2 and $(CH_3)_2NPH_2$ are *not* due to some geometrical relationship between the *phosphorus* lone pair and the vicinal hydrogens, but rather must be due to the lone pairs on *oxygen and nitrogen*, which are not present in $(CH_3)_3CPH_2$. These results suggest that at least some of the problems reported for fitting Karplus curves to PNCH moieties[19,46,47] arise due to variations in nitrogen pyramidalization and perhaps non-Karplus effects on $^3J_{PH}$ due to the nitrogen lone pair.

In an attempt to briefly assess the nitrogen lone pair effect, the conformation of $(CH_3)_2NPH_2$ with the largest value of $^3J_{PH}$ = 49 Hz at θ,ω = 180°, 30° was minimized following inversion at nitrogen but keeping θ and ω fixed. Calculation of the coupling constant gave $^3J_{PH}$ = 42 Hz at the same θ,ω = 180°, 30°, so the effect is modest. The local energy minimum of this structure was 4.3 kcal/mol higher, so it is possible that the changes in bond angles and distances could have as much effect on the change in coupling constant as the change in nitrogen lone pair position; since the effect was in any event a small fraction of the initial coupling constant, the potential non-Karplus effect is clearly smaller than that due to the phosphorus lone pair.

The overall shapes of the θ,ω surfaces are similar, exhibiting a maximum in $^3J_{PH}$ near θ = 180° and ω = 0°, a secondary maximum near θ = 0° and ω = 0°, and troughs near θ = ± 90° as well as at ω = 180°; these features can be seen in Figure 6. Since the minimum near θ = ± 90° is relatively independent of ω, this can account for the observation of "normal" Karplus behavior in trivalent phosphorus compounds.[6−8,18,19] Experimentally, as has been noted in the literature,[19−32] the highest vicinal coupling constants occur for hydrogen anti to phosphorus (i.e., θ = 180°) and the lone pair gauche to the CH carbon (i.e., ω = 60°). For CH_3OPH_2, the highest coupling constant is indeed at θ = 180° and the lone pair eclipsing the CH carbon (i.e., ω = 0°); at ω = ± 60°, $^3J_{PH}$ is still ∼80% of the calculated maximum value of 43.4 Hz. This effect was seen for **5** where $^3J_{PH}$ = 19 Hz, as well as for **2** and **3** where the rotationally averaged coupling was ∼20 Hz for the gauche methyl groups, and readily accounted for by the existence of a ∼45 Hz anti coupling constant.

Our examples of coupling of phosphorus to the ring hydrogen atoms of heterocycles **6** and **7** exhibit values in and near the θ,ω troughs, including relatively small positive and negative values of $^3J_{PH}$. While the consensus in the literature is that PNCH dihedral angles are not reliable for use in determining stereochemistry,[19,46,47] our results show that the variability is due to small dihedral angle differences and the asymmetry of the troughs that can give different coupling constants at similar Karplus angles (i.e., ± θ), as demonstrated by the non-Karplus result of **7c**. As seen in Figure 6b where $^3J_{PH}$ is plotted at ω = 225.9°, corresponding to the planar heterocycle structure (Figure 5c), that asymmetry leads to the larger cis coupling constant for θ = 120° and the small negative trans coupling constant for θ = 240° (or −120°). For the nonplanar heterocycles **6**, those angles are near 135° and −100° for cis and trans, respectively (see Table S-2 in the Supporting Information for DFT and X-ray values for **6a** and **6c**), and as seen from Figure 6b these would be expected to give qualitatively similar coupling constant values to those seen at θ = ± 120°.

CONCLUSION

An obvious question is whether the observed dependence of vicinal coupling on a non-Karplus angle is unique. Some work on $^3J_{HH}$ and $^3J_{CH}$ has been reported but with much smaller observed secondary dependencies on the vicinal coupling constants than seen for $^3J_{PH}$ on ω.[67−71] Given the ubiquity of the Karplus method, it is likely that the strong dependence of $^3J_{PH}$ on a non-Karplus angle is indeed novel.

Another obvious question is whether the effort to create a two-dimensional Karplus equation for $^3J_{PH}$ is warranted. Unless a specific system will be evaluated repeatedly at different θ and ω torsional angles, the answer clearly is no, since the detailed values are dependent on the intervening atoms and the atoms attached to phosphorus. With the increasing ease of use of computer programs to calculate coupling constants using density functional methods, it is reasonably fast and accurate to carry out a DFT calculation on the desired system, without compromising on the choice of atoms, and this point has been made with force in a recent review article.[72] The two-dimensional Karplus method might have utility for molecules too large to allow a high-level DFT calculation to be carried out, yet small enough to allow a lower-level structure optimization to give good values for θ and ω.

The results provide a number of examples of the power of theoretical NMR methods.[72−77] At the most concrete level, we have provided an analytical solution to a long-standing problem, in which it was recognized that lone pair conformation had an effect on vicinal phosphorus−hydrogen coupling constants, but not that the interplay of the lone pair conformation and the "normal" Karplus angle could yield coupling constants ranging from −4 to +51 Hz, as shown here, with the maximum for a PYCH dihedral angle of 180° and a lone pair-PYC dihedral angle of 0°. Equally importantly, the results show how theoretical calculations of structure and NMR chemical shifts and coupling constants can provide, for instance, an explanation of temperature-dependent chemical shifts (here on the basis of equilibrating sulfonamide conformations) and independent confirmation of NMR assignments, as in the methyl group assignments in **2** and the stereochemical assignments in **6c** and **7c**. The methods described here have general utility in organic structure determination, and we join those who recommend that they be considered as necessary adjuncts to experimental determination of NMR data.[72−77]

EXPERIMENTAL SECTION

General. All manipulations of air-sensitive compounds were carried out in an inert atmosphere glovebox under recirculating nitrogen. ^{1}H, ^{13}C, and ^{31}P NMR spectra were recorded at 400, 100, and 160 MHz, respectively; chemical shifts are reported relative to TMS for ^{1}H and ^{13}C NMR, and to external 85% H_3PO_4 at 0 ppm (positive values downfield) for ^{31}P NMR. Infrared spectra were obtained in 0.1 mm NaCl solution cells on a computer-controlled FT-IR spectrometer. All solvents were treated under nitrogen. Tetrahydrofuran was distilled from sodium benzophenone ketyl. $CDCl_3$ was vacuum-transferred from phosphorus pentoxide. $PhPCl_2$ was degassed prior to use and NEt_3 was distilled from CaH_2. Simulations of NMR spectra were carried out using *gNMR v3.6* (Cherwell Scientific) on a Macintosh computer; while this version is no longer commercially available, a non-commercial version is available at http://home.cc.umanitoba.ca/~budzelaa/gNMR/gNMR.html under the terms described there.

5-Oxo-2-phenyl-3-*p*-toluenesulfonyl-1,3,2-oxazaphospholidine (6c). In the glovebox, a solution of 1.10 g of $PhPCl_2$ (6.14 mmol) in ∼1 mL of THF was added to a well-stirred solution of 1.56 g

dx.doi.org/10.1021/jo3003776 | J. Org. Chem. 2012, 77, 4968−4979

Table 3. Variable Temperature NMR Data[a]

T (°C)	ν_{trans}	ν_{trans} (calcd)[b]	ν_{cis}	ν_{cis} (calcd)[b]	$\nu_{1/2}$ (TMS)	$^2J_{HH}$[c]	$^3J_{PH(cis)}$[c]	$\Delta\nu_{obs}$	$\Delta\nu_{calcd}$
−40	1574.81	1574.60	1546.04	1545.66	1.40	17.53	3.77	28.8	28.9
−20	1565.47	1565.76	1542.48	1542.85	1.23	17.48	3.88	23.0	22.9
0	1556.90	1556.93	1539.68	1540.03	1.78	17.51	3.80	17.2	16.9
23	1546.88	1546.77	1537.13	1536.79	0.84	17.53	4.11	9.8	10.0
50	1536.5[d]	1534.84	1534.3[d]	1532.99	1.08	17.5[d]	3.8[d]	2.2	1.85

[a]All values for chemical shifts (ν) and coupling constants (J) in Hz; spectrometer frequency is 400.13 MHz. [b]Linear fit to values from −40 to +23 °C. [c]Best fit value from NMR iteration using observed frequencies and peak heights, setting $^3J_{PH(trans)} = -1$ Hz. [d]The calculated chemical shifts were clearly in error by ∼1.5 Hz, albeit in the same direction, so these values were fit to the observed spectra, using the coupling constants previously determined ($^2J_{HH}$ =17.5 Hz, $^3J_{PH(cis)}$ = 3.8 Hz, and $^3J_{PH(trans)}$ = −1 Hz).

of Et_3N (15.4 mmol) and 1.01 g of *N*-*p*-toluenesulfonylglycine[78] (4.42 mmol) in 30 mL of THF. A white precipitate of $Et_3NH^+Cl^-$ formed immediately, and after ∼2 min a heterogeneous sample was removed and a few drops added to $CDCl_3$ for ^{31}P NMR analysis, showing the reaction to be complete. The white suspension started to turn brown and was filtered through a pad of Celite. The solvent was removed in vacuo to give 1.09 g (73% yield) of a sticky brown solid; in several experiments yields ranging from 61% to 81% were typically obtained, containing ∼8 mol % (3% by weight) of $Et_3NH^+Cl^-$. The crude material was dissolved in 2 mL of CH_2Cl_2 and cooled to −30 °C, and 4 mL of ether was layered on. After standing overnight at −30 °C, light brown crystals were obtained, but they were enriched in $Et_3NH^+Cl^-$. Solvent removal from the filtrate gave a dark brown solid that, while depleted in $Et_3NH^+Cl^-$, contained impurities as judged by ^1H NMR and was discarded. The brown crystals were recrystallized as before, but from 3 mL of a 1:2 mixture of CH_2Cl_2 and ether, to give light brown crystals that were similarly enriched in $Et_3NH^+Cl^-$, and a filtrate that gave a small amount of light yellow solid that consisted of **6c** and only a trace of $Et_3NH^+Cl^-$. Recrystallization of this material from 3 mL of a 1:2 mixture of CH_2Cl_2 and ether gave 0.09 g of pure **6c** as white crystals (6% yield): mp 102−103 °C; IR ($CHCl_3$) 3008, 2925, 1797, 1357, 1169 cm^{-1}; ^1H NMR ($CDCl_3$) δ 7.79 (d, J = 8.4 Hz, 2H), 7.59 (m, 2 H), 7.51 (m, 3H), 7.36 (d, J = 8.4 Hz, 2H), 3.86 (ABX, 2H, see text), 2.46 (s, 3H); ^{31}P NMR ($CDCl_3$) 136.3 ppm; ^{13}C NMR ($CDCl_3$, assignments from 2D HETCOR) 170.5 (d, $^2J_{PC}$ = 13.5 Hz), 145.2, 138.2 (d, $^1J_{PC}$ = 38.7 Hz), 134.8, 132.2 (Ph C_4, coupled to ^1H δ7.51), 130.3 (tolyl CH, coupled to ^1H δ7.36), 129.2 (d, $^2J_{PC}$ = 6.0 Hz, Ph C_3, coupled to ^1H δ7.51), 129.1 (d, J_{PC} = 22.2 Hz, Ph C_2, coupled to ^1H δ7.59), 127.4 (d, J_{PC} = 2.6 Hz, tolyl CH, coupled to ^1H δ7.79), 43.7, 21.7 ppm. Anal. Calcd for $C_{15}H_{14}NO_4SP$: C, 53.73; H, 4.21; N, 4.18. Found: C, 53.40; H, 4.08; N, 4.06.

Variable Temperature NMR Spectra. A 10-mg sample of **6c** was dissolved in $CDCl_3$ (∼0.5 mL) with 1% TMS as the non-exchanging reference peak. Observed and calculated data are collected in Table 3. Simulation of the NMR spectra using these data was carried out using *gNMR*, and the best fit values were determined by visual comparison of the observed and simulated spectra.

NMR Calculations. Calculations were carried out using *Gaussian 03W* Revision B.03, C.01, and D.01 as well as *Gaussian 09* Revision A.02;[48] numerical results with each revision were the same. The latter versions of *03W* are required to calculate only specified coupling constants and to implement (for example) the uTZ-w method described in the text using keywords and overlays nmr=(giao,mixed,spinspin) IOp(3/75=199590,10/48=10) cphf(conver=10) integral(grid=ultrafine), while *09* allows this without the overlays; atom numbers for the spin−spin calculation are input as a free format list after the molecule specification.[53,79] Solvent modeling[73,76] using SCRF calculations for chloroform (IEFPCM) were used for the sulfonamide and *t*-Boc rotations in **6c** and **7b**, **7c**, respectively, and had negligible effect on coupling constants; no significant effect was seen using solvent modeling for CH_3OPH_2. Use of the solvent modeling did lead to small changes in energies of conformations as well as, it seemed, a flatter energy surface with more local minima, an effect previously seen.[80] A frequency calculation was performed for all minima found, and all gave positive frequencies indicative of local minima. Energies and coordinates may be found in the Supporting Information.

■ ASSOCIATED CONTENT

Supporting Information

Tables of X-ray and calculated structural data for **2**, **3**, **6a**, **6c$_1$**, **6c$_2$**, *syn*-**6c**, **7a**, **7b**, **7c**, *E*-**7c$_1$**, *E*-**7c$_2$**; XYZ coordinates and energies of optimized structures of **2**, **3**, **6a**, **6c$_1$**, **6c$_2$**, *syn*-**6c**, **7b**, (*E*)-**7b**, **7c**, *E*-**7c$_1$**, *E*-**7c$_2$**, CH_3OPH_2, $(CH_3)_2NPH_2$, $(CH_3)_3CPH_2$; details of the DFT calculations for $(CH_3)_2NPH_2$ and $(CH_3)_3CPH_2$; details of the derivation of the 2-D Karplus equations; tables of calculated $^3J_{PH}$ (DFT and Karplus equation) and relative energies versus θ,ω for CH_3OPH_2, $(CH_3)_2NPH_2$, and $(CH_3)_3CPH_2$; NMR and IR spectra of **6c**. This material is available free of charge via the Internet at http://pubs.acs.org.

■ AUTHOR INFORMATION

Corresponding Author

*E-mail: william.hersh@qc.cuny.edu.

Notes

The authors declare no competing financial interest.

■ ACKNOWLEDGMENTS

We thank the National Institutes of Health (GM59596-01) and the City University of New York PSC-CUNY Research Award Program for financial support of this work and Jerome Schulman, Cherice Evans, Joseph Dannenberg, and Fernando Clemente for assistance with *Gaussian*.

■ REFERENCES

(1) Karplus, M. *J. Chem. Phys.* **1959**, *30*, 11−15.
(2) Karplus, M. *J. Am. Chem. Soc.* **1963**, *85*, 2870−2871.
(3) Benezra, C.; Ourisson, G. *Bull. Soc. Chim. Fr.* **1966**, 1825−1827.
(4) Benezra, C. *J. Am. Chem. Soc.* **1973**, *95*, 6890−6894.
(5) Bothner-By, A. A.; Cox, R. H. *J. Phys. Chem.* **1969**, *73*, 1830−1834.
(6) Kainosho, M.; Nakamura, A. *Tetrahedron* **1969**, *25*, 4071−4081.
(7) White, D. W.; Verkade, J. G. *J. Magn. Reson.* **1970**, *3*, 111−116.
(8) Bergesen, K.; Albriktsen, P. *Acta Chem. Scand.* **1971**, *25*, 2257−2263.
(9) Blackburn, B. J.; Lapper, R. D.; Smith, I. C. P. *J. Am. Chem. Soc.* **1973**, *95*, 2873−2878.
(10) Lee, C.-H.; Sarma, R. H. *J. Am. Chem. Soc.* **1976**, *98*, 3541−3548.
(11) Lankhorst, P. P.; Haasnoot, C. A. G.; Erkelens, C.; Altona, C. *J. Biomol. Struct. Dyn.* **1984**, *1*, 1387−1405.
(12) Gorenstein, D. G. *Chem. Rev.* **1994**, *94*, 1315−1338.
(13) Ojha, R. P.; Dhingra, M. M.; Sarma, M. H.; Shibata, M.; Farrar, M.; Turner, C. J.; Sarma, R. H. *Eur. J. Biochem.* **1999**, *265*, 35−53.
(14) Oikawa, M.; Shintaku, T.; Yoshizaki, H.; Fukase, K.; Adachi, S.; Lee, K.; Kusumoto, S. *Bull. Chem. Soc. Jpn.* **2001**, *74*, 1455−1461.
(15) Sakamoto, Y.; Kondo, K.; Onozato, M.; Aoyama, T. *Polycyclic Aromat. Compd.* **2006**, *26*, 59−68.

(16) Giessner-Prettre, C.; Pullman, B. *J. Theor. Biol.* **1974**, *48*, 425−443.
(17) Giessner-Prettre, C.; Pullman, B. *J. Theor. Biol.* **1978**, *72*, 751−756.
(18) Quin, L. D.; Gallagher, M. J.; Cunkle, G. T.; Chesnut, D. B. *J. Am. Chem. Soc.* **1980**, *102*, 3136−43.
(19) Huang, Y.; Arif, A. M.; Bentrude, W. G. *J. Org. Chem.* **1993**, *58*, 6235−6246.
(20) Gagnaire, D.; Robert, J. B.; Verrier, J. *Bull. Soc. Chim. Fr.* **1966**, 3719−25.
(21) Gagnaire, D.; Robert, J. B. *Bull. Soc. Chim. Fr.* **1967**, 2240−2241.
(22) Gagnaire, D.; Robert, J. B.; Verrier, J. *Bull. Soc. Chim. Fr.* **1968**, 2392−2400.
(23) Cowley, A. H.; Dewar, M. J. S.; Jackson, W. R.; Jennings, W. B. *J. Am. Chem. Soc.* **1970**, *92*, 1085−1086.
(24) Albrand, J.-P.; Gagnaire, D.; Picard, M.; Robert, J.-B. *Tetrahedron Lett.* **1970**, *11*, 4593−4596.
(25) Robert, J. B.; Roberts, J. D. *J. Am. Chem. Soc.* **1972**, *94*, 4902−4904.
(26) Bushweller, C. H.; Brunelle, J. A.; Anderson, W. G.; Bilofsky, H. S. *Tetrahedron Lett.* **1972**, *13*, 3261−3264.
(27) Bentrude, W. G.; Tan, H. W. *J. Am. Chem. Soc.* **1972**, *94*, 8222−8224.
(28) Bentrude, W. G.; Tan, H.-W. *J. Am. Chem. Soc.* **1973**, *95*, 4666−4675.
(29) Bentrude, W. G.; Tan, H.-W.; Yee, K. C. *J. Am. Chem. Soc.* **1975**, *97*, 573−582.
(30) Bentrude, W. G.; Setzer, W. N. Stereospecificity in ^{31}P-Element Couplings: Proton-Phosphorus Couplings. In *Phosphorus-31 NMR Spectroscopy in Stereochemical Analysis*; Verkade, J. G., Quin, L. D., Eds.; VCH Publishers, Inc.: Deerfield Beach, 1987; pp 365−389.
(31) Bentrude, W. G. Use of J_{HP} Values to Determine the Conformations of Saturated Six-Membered Rings Containing Phosphorus. In *Phosphorus-31 NMR Spectral Properties in Compound Characterization and Structural Analysis*; Quin, L. D., Verkade, J. G., Eds.; VCH Publishers, Inc.: New York, 1994; pp 41−53.
(32) Huang, Y.; Yu, J.; Bentrude, W. G. *J. Org. Chem.* **1995**, *60*, 4767−4773.
(33) Gil, V. M. S.; Philipsborn, W. V. *Magn. Reson. Chem.* **1989**, *27*, 409−430.
(34) Hersh, W. H.; Xu, P.; Simpson, C. K.; Wood, T.; Rheingold, A. L. *Inorg. Chem.* **1998**, *37*, 384−385.
(35) Hersh, W. H.; Klein, L.; Todaro, L. J. *J. Org. Chem.* **2004**, *69*, 7355−7358.
(36) Hersh, W. H.; Xu, P.; Simpson, C. K.; Grob, J.; Bickford, B.; Hamdani, M. S.; Wood, T.; Rheingold, A. L. *J. Org. Chem.* **2004**, *69*, 2153−2163.
(37) Garrigues, B.; Munoz, A.; Koenig, M.; Sanchez, M.; Wolf, R. *Tetrahedron* **1977**, *33*, 635−643.
(38) Munoz, A.; Garrigues, B.; Wolf, R. *Phosphorus Sulfur* **1978**, *4*, 47−52.
(39) Lamande, L.; Munoz, A. *Phosphorus, Sulfur Silicon* **1993**, *75*, 241−244.
(40) Fu, H.; Tu, G.-Z.; Li, Z.-L.; Zhao, Y.-F.; Zhang, R.-Q. *J. Chem. Soc., Perkin Trans. 1* **1997**, 2021−2022.
(41) Zhang, N. J.; Lu, H. Y.; Chen, X.; Zhao, Y.-F. *Synthesis* **1998**, 376−378.
(42) Fu, H.; Tu, G.-Z.; Li, Z.-L.; Zhao, Y.-F. *Synthesis* **1998**, 855−858.
(43) Lu, K.; Tu, G.-Z.; Guo, X.-F.; Sun, X.-B.; Liu, Y.; Feng, Y.-P.; Zhao, Y.-F. *J. Mol. Struct.* **2002**, *610*, 65−72.
(44) Eliel, E. L.; Wilen, S. H.; Mander, L. N. In *Stereochemistry of Organic Compounds*; Wiley-Interscience: New York, 1994; pp 541−542.
(45) Setzer, W. N.; Black, B. G.; Hovanes, B. A.; Hubbard, J. L. *J. Org. Chem.* **1989**, *54*, 1709−1713.
(46) Schwalbe, C. H.; Chopra, G.; Freeman, S.; Brown, J. M.; Carey, J. V. *J. Chem. Soc., Perkin Trans. 2* **1991**, 2081−2090.
(47) Hutchins, R. O.; Maryanoff, B. E.; Albrand, J. P.; Cogne, A.; Gagnaire, D.; Robert, J. B. *J. Am. Chem. Soc.* **1972**, *94*, 9151−9158.
(48) Frisch, M. J.; Trucks, G. W.; Schlegel, H. B.; Scuseria, G. E.; Robb, M. A.; Cheeseman, J. R.; Scalmani, G.; Barone, V.; Mennucci, B.; Petersson, G. A.; Nakatsuji, H.; Caricato, M.; Li, X.; Hratchian, H. P.; Izmaylov, A. F.; Bloino, J.; Zheng, G.; Sonnenberg, J. L.; Hada, M.; Ehara, M.; Toyota, K.; Fukuda, R.; Hasegawa, J.; Ishida, M.; Nakajima, T.; Honda, Y.; Kitao, O.; Nakai, H.; Vreven, T.; Montgomery, Jr., J. A.; Peralta, J. E.; Ogliaro, F.; Bearpark, M.; Heyd, J. J.; Brothers, E.; Kudin, K. N.; Staroverov, V. N.; Kobayashi, R.; Normand, J.; Raghavachari, K.; Rendell, A.; Burant, J. C.; Iyengar, S. S.; Tomasi, J.; Cossi, M.; Rega, N.; Millam, N. J.; Klene, M.; Knox, J. E.; Cross, J. B.; Bakken, V.; Adamo, C.; Jaramillo, J.; Gomperts, R.; Stratmann, R. E.; Yazyev, O.; Austin, A. J.; Cammi, R.; Pomelli, C.; Ochterski, J. W.; Martin, R. L.; Morokuma, K.; Zakrzewski, V. G.; Voth, G. A.; Salvador, P.; Dannenberg, J. J.; Dapprich, S.; Daniels, A. D.; Farkas, Ö.; Foresman, J. B.; Ortiz, J. V.; Cioslowski, J.; Fox, D. J. *Gaussian 03, Revision D.01 and Gaussian 09, Revision A.02*; Gaussian, Inc.: Wallingford, CT, 2009.
(49) Foresman, J. B.; Frisch, Æ. *Exploring Chemistry with Electronic Structure Methods*, 2nd ed.; Gaussian, Inc.: Pittsburgh, 1996; p 52.
(50) Cheeseman, J. R.; Frisch, Æ. *Technical Support Information: Predicting Magnetic Properties with ChemDraw and Gaussian*. http://www.gaussian.com/g_whitepap/nmrcomp.htm.
(51) Salvador, P.; Dannenberg, J. J. *J. Phys. Chem. B* **2004**, *108*, 15370−15375.
(52) Tähtinen, P.; Bagno, A.; Koch, A.; Pihlaja, K. *Eur. J. Org. Chem.* **2004**, 4921−4930.
(53) Deng, W.; Cheeseman, J. R.; Frisch, M. J. *J. Chem. Theory Comput.* **2006**, *2*, 1028−1037.
(54) Subramaniam, G.; Hersh, W. H., unpublished work.
(55) Jensen, F. *J. Chem. Theory Comput.* **2006**, *2*, 1360−1369.
(56) Elguero, J.; Goya, P.; Rozas, I.; Catalán, J.; De Paz, J. L. G. *J. Mol. Struct. (THEOCHEM)* **1989**, *184*, 115−129.
(57) Bindal, R. D.; Golab, J. T.; Katzenellenbogen, J. A. *J. Am. Chem. Soc.* **1990**, *112*, 7861−7868.
(58) Nicholas, J. B.; Vance, R.; Martin, E.; Burke, B. J.; Hopfinger, A. J. *J. Phys. Chem.* **1991**, *95*, 9803−9811.
(59) Nyulászi, L.; Szieberth, D.; Csonka, G. I.; Réffy, J.; Heinicke, J.; Veszprémi, T. *Struct. Chem.* **1995**, *6*, 1−7.
(60) Kolehmainen, E.; Gawinecki, R.; Ośmiałowski, B., NMR Spectra of Anilines. In *The Chemistry of Anilines, Part 1*; Rappoport, Z., Ed.; John Wiley & Sons Ltd.: Chichester, England, 2007; pp 347−371.
(61) Dréan, P.; Le, G. M.; López, J. C.; Alonso, J. L.; Denis, J. M.; Kreglewski, M.; Demaison, J. *J. Mol. Spectrosc.* **1994**, *166*, 210−23.
(62) Egan, W.; Mislow, K. *J. Am. Chem. Soc.* **1971**, *93*, 1805−1806.
(63) Yavari, I.; Hadigheh-Rezvan, V. *Phosphorus, Sulfur Silicon Relat. Elem.* **2001**, *174*, 151−162.
(64) Jugé, S.; Stephan, M.; Genet, J. P.; Halut-Desportes, S.; Jeannin, S. *Acta Crystallogr.* **1990**, *C46*, 1869−1872.
(65) Baechler, R. D.; Mislow, K. *J. Am. Chem. Soc.* **1970**, *92*, 3090−3093.
(66) Mukhlall, J. A.; Hersh, W. H. *Inorg. Chim. Acta* **2011**, *369*, 62−70.
(67) Thibaudeau, C.; Stenutz, R.; Hertz, B.; Klepach, T.; Zhao, S.; Wu, Q.; Carmichael, I.; Serianni, A. S. *J. Am. Chem. Soc.* **2004**, *126*, 15668−15685.
(68) Klepach, T. E.; Carmichael, I.; Serianni, A. S. *J. Am. Chem. Soc.* **2005**, *127*, 9781−9793.
(69) Zhao, H.; Pan, Q.; Zhang, W.; Carmichael, I.; Serianni, A. S. *J. Org. Chem.* **2007**, *72*, 7071−7082.
(70) Mobli, M.; Almond, A. *Org. Biomol. Chem.* **2007**, *5*, 2243−2251.
(71) Hu, X.; Carmichael, I.; Serianni, A. S. *J. Org. Chem.* **2010**, *75*, 4899−4910.
(72) Bifulco, G.; Dambruoso, P.; Gomez-Paloma, L.; Riccio, R. *Chem. Rev.* **2007**, *107*, 3744−3779.
(73) Jain, R.; Bally, T.; Rablen, P. R. *J. Org. Chem.* **2009**, *74*, 4017−4023.

(74) Di Micco, S.; Chini, M. G.; Riccio, R.; Bifulco, G. *Eur. J. Org. Chem.* **2010**, *2010*, 1411−1434.
(75) Saielli, G.; Nicolaou, K. C.; Ortiz, A.; Zhang, H.; Bagno, A. *J. Am. Chem. Soc.* **2011**, *133*, 6072−6077.
(76) Bally, T.; Rablen, P. R. *J. Org. Chem.* **2011**, *76*, 4818−4830.
(77) López-Vallejo, F.; Fragoso-Serrano, M.; Suárez-Ortiz, G. A.; Hernández-Rojas, A. C.; Cerda-García-Rojas, C. M.; Pereda-Miranda, R. *J. Org. Chem.* **2011**, *76*, 6057−6066.
(78) McChesney, E. W.; Swann, W. K. J. *J. Am. Chem. Soc.* **1937**, *59*, 1116−1118.
(79) Clemente, F. R. Personal Communication, Technical Support, Gaussian, Inc. 2008.
(80) Mukhlall, J. A.; Noll, B. C.; Hersh, W. H. *J. Sulfur Chem.* **2011**, *32*, 199−212.